

Control of the Graphene–Protein Interface Is Required To Preserve Adsorbed Protein Function

Thomas Alava,^{*,†} Jason A. Mann,[‡] Cécile Théodore,[†] Jaime J. Benitez,[†] William R. Dichtel,^{*,‡} Jeevak M. Parpia,[§] and Harold G. Craighead[†]

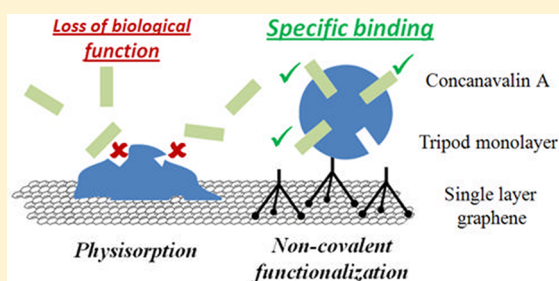
[†]School of Applied and Engineering Physics, Cornell University, Ithaca, New York 14853, United States

[‡]Department of Chemistry and Chemical Biology, Baker Laboratory, Cornell University, Ithaca, New York 14853, United States

[§]Laboratory of Atomic and Solid-State Physics, Cornell University, Ithaca, New York 14853, United States

S Supporting Information

ABSTRACT: Graphene's suite of useful properties makes it of interest for use in biosensors. However, graphene interacts strongly with hydrophobic components of biomolecules, potentially altering their conformation and disrupting their biological activity. We have immobilized the protein Concanavalin A onto a self-assembled monolayer of multivalent tripodal molecules on single-layer graphene. We used a quartz crystal microbalance (QCM) to show that tripod-bound Concanavalin A retains its affinity for polysaccharides containing α -D-glucopyranosyl groups as well as for the α -D-mannopyranosyl groups located on the cell wall of *Bacillus subtilis*. QCM measurements on unfunctionalized graphene indicate that adsorption of Concanavalin A onto graphene is accompanied by near-complete loss of these functions, suggesting that interactions with the graphene surface induce deleterious structural changes to the protein. Given that Concanavalin A's tertiary structure is thought to be relatively robust, these results suggest that other proteins might also be denatured upon adsorption onto graphene, such that the graphene–biomolecule interface must be considered carefully. Multivalent tripodal binding groups address this challenge by anchoring proteins without loss of function and without disrupting graphene's desirable electronic structure.



Single-layer graphene (SLG) is mechanically flexible, transparent, and conductive, and it offers outstanding surface-to-volume ratio.¹ These properties make SLG of interest for integrated lab-on-a-chip analysis systems, particularly when it is functionalized with appropriate biosensing elements. For example, SLG has been incorporated into electrolyte-gated field effect transistors,² and SLG–aptamer interactions have served as active elements of a Förster resonance energy transfer-based thrombin sensor.³ McAlpine and co-workers recently developed an implantable, wireless biosensor based on SLG functionalized with graphene-binding peptides.⁴ Aromatic portions of biomolecules can interact with graphene's polarizable, hydrophobic surface. For example, the nucleobases of single-stranded DNA (ssDNA) adsorb strongly onto the graphene basal plane, and the ssDNA retains its ability to hybridize with a complementary strand.^{5,6}

In contrast, proteins, which constitute the largest and most widely employed class of biomacromolecules for surface functionalization,^{7–11} have also been interfaced to graphene,^{2,12} but most studies do not unambiguously demonstrate that the protein remains functional.^{13,14} The nature and magnitude of protein tertiary structure distortion upon adsorption onto a hydrophobic surface is dependent on many factors, including the number of nonpolar amino acids and the energetics of the equilibrium between folded and denatured states.^{15,16} So-called

“soft” proteins, with less-stable tertiary structures, undergo larger deformations.¹⁷ Tertiary structure changes also depend upon the nature of the sorbent. For example, the α -helix content of cutinase and α -chymotrypsin decrease when bound to hydrophobic SiO₂, yet their biological activity is mostly maintained. However, a similar decrease in α -helix content occurs upon adsorption to Teflon, but catalytic activity is lost.¹⁸ Hydrophobic effects were also ascribed to lysozyme and α -lactalbumin denaturation on polystyrene.¹⁹ Meanwhile, early studies have suggested changes in peptide secondary structure upon adsorption to SLG.²⁰ These findings suggest that many proteins might undergo conformational changes, perhaps accompanied by loss of function, when adsorbed nonspecifically onto SLG.

In light of this concern, here we characterize and engineer the nature of the SLG–protein interface for a model lectin protein, Concanavalin A (Con A). We first employ a graphene-coated quartz crystal microbalance (GQCM) to characterize the immobilization of Con A on SLG. We interfaced Con A to SLG in two distinct ways: either (1) adsorbed to its pristine

Received: November 9, 2012

Accepted: January 31, 2013

Published: January 31, 2013



basal plane or (2) covalently attached to a self-assembled monolayer (SAM) of tripodal molecules bearing an activated ester for bioconjugation. We have previously demonstrated that these tripodal compounds bind strongly to graphene, even in organic solvents under infinite dilution conditions,²¹ and diffuse in two-dimensions over the graphene surface.²² In parallel, we have also found that antibodies attached to tripod monolayers exhibit highly specific biological recognition, while those bound to bare graphene or through a monovalent pyrene anchor lose this hallmark ability.²³

After characterizing Con A adsorption onto graphene, we assessed its well-known ability to recognize α -D-glucopyranose moieties of oligosaccharides. Con A retains activity when attached to the tripod monolayer but shows no evidence of specific oligosaccharide recognition when adsorbed onto pristine SLG. Furthermore, Con A recognizes the α -D-mannopyranose moieties of the lipotechoic acids located on *Bacillus subtilis* cell walls. We evaluated SLG-immobilized Con A's ability to recognize *B. subtilis* by measuring the density of immobilized cells. Finally, we demonstrate that it is possible to inhibit recognition of cells by presaturating the Con A receptors with methyl- α -D-mannopyranose. These experiments confirm that Con A remains fully functional when attached to the tripod SAM and suggest that the tripod will provide a general strategy for interfacing biomolecules to SLG. This study also demonstrates the utility of QCM with motional resistance monitoring to characterize the interactions of biomacromolecules with SLG.

■ EXPERIMENTAL SECTION

Graphene Transfer. SLG was grown on Cu substrates (Alfa Aesar, Ward Hill, MA) in an atmosphere of CH₄ (36 sccm) and H₂ (60 sccm) at 980 °C for 30 min.²⁴ A 50 nm layer of poly(methyl methacrylate) (PMMA) was spin-coated onto the SLG, after which the Cu substrate was etched using aqueous FeCl₃ (1 M, Transene, Danvers, MA). The SLG/PMMA was transferred into three fresh baths of deionized H₂O. Finally, the SLG/PMMA was transferred, SLG side down, onto a substrate, either a quartz crystal (referred to as QCM) or a silicon wafer with a thermally grown 280 nm-thick SiO₂ layer (Si/SiO₂, for cell immobilization studies). The SiO₂ layer provides sufficient optical contrast to visualize the SLG directly.²⁵ After deposition, the SLG was dried for 3 h, after which the PMMA was removed by soaking the substrate in anisole for 15 min and then CH₂Cl₂ for 12 h. The SLG was found to be continuous and predominantly single layer (>95%) using Raman spectroscopy (see Supporting Information).

Reagents. Con A from *Canavalia ensiformis* (Jack bean, Sigma Aldrich, Saint Louis, MO) was dissolved in phosphate-buffered saline 1X solution (PBS 1X, 10 mM, pH 7.3) to a concentration of 200 μ g mL⁻¹. Working solutions of Con A were prepared from the aliquots before the beginning of each experiment by dissolving the protein in PBS 1X to a concentration of 50 μ g mL⁻¹. Guanadinium hydrochloride, α -D-glucose, propidium iodine, methyl α -D-mannopyranoside, and lysogeny broth (LB) were purchased from Sigma Aldrich. Saturated solutions of polysaccharides containing α -D-glucopyranose moieties with the proper configuration to be recognized by Con A²⁶ were prepared according to a reported procedure,²⁷ diluted by a factor 1:2 in PBS 1X, and stored at 4 °C until use (see Supporting Information). Propidium iodine was dissolved in deionized H₂O (500 μ g mL⁻¹). Solutions of *B. subtilis* were prepared by inoculating 5 mL of LB medium with an overnight

culture of *B. subtilis* under sterile conditions. The inoculated media was incubated under an aerobic atmosphere with 6.5% CO₂ with constant shaking until the optical density at 600 nm (OD₆₀₀) reached 0.6, corresponding to mid-log phase growth. The *B. subtilis* cells were resuspended in PBS1 X and diluted to a concentration of 10⁸ cfu mL⁻¹. *B. subtilis* concentrations were estimated using a hemacytometer.

Noncovalent Functionalization Protocol. Monolayers of the *N*-hydroxysuccinimidyl ester tripod (NHS-tripod) were formed by submerging the SLG-functionalized substrate into a solution of NHS-tripod in THF (100 μ M) for 1 min. The substrate was rinsed with fresh THF and was then submerged in deionized H₂O for 1 min. The synthesis of the NHS-tripod is described elsewhere.²³

Cell Surface Density Counting. Graphene supported on the Si/SiO₂ wafers, with or without a tripod monolayer, was functionalized with Con A by spreading a 100 μ L droplet evenly to cover the entire graphene sample (ca. 1 cm²). After incubation, the sample was rinsed gently with PBS 1X (3 \times 1 mL). Care was taken to ensure that the samples did not dry during the functionalization and subsequent bacterial recognition procedures. α -D-Mannopyranose solution (inhibition solution) or 6 M guanadinium hydrochloride (denaturant solution) was introduced to the SLG surface using a similar procedure. Finally, graphene samples were incubated for 20 min in a solution of *B. subtilis* resuspended in PBS 1X (5 mL, 1 \times 10⁸ cfu mL⁻¹), rinsed thoroughly three times with PBS 1X, and dried under a stream of N₂. The attached bacteria were counted by depositing aqueous propidium iodide (20 μ L, 500 μ g mL⁻¹) over the samples and incubating under a glass slide for 45 min. An Olympus AX-70 microscope equipped with a Photometrics Cascade II EMCCD camera was used to image the resulting surfaces and determine the bound cell density.

Quartz Crystal Microbalance. SLG-functionalized quartz substrates were inserted into a Kynar crystal holder (Stanford Research Systems (SRS), model O100RH) equipped with a flow cell (SRS model O100FC) and peristaltic pump (Gilson, Middleton, WI). Stable temperatures were maintained by submerging the crystal holder in a controlled-temperature water bath at 27 °C (Thermo Scientific, Precision 280 series, temperature uniformity of \pm 0.2 °C at 27 °C). Solutions were pumped over the active SLG substrate using a flow rate of 30 μ L min⁻¹. The quartz holder electrodes were connected to a controller interface (SRS, model QCM-200) delivering the resonance frequency and the motional resistance signal. Once acquired, the data are treated to remove baseline drift and external vibration artifacts (see Supporting Information). Throughout the article, representative QCM resonance frequency and motional resistance curves are displayed, and numerical data are reported as the mean of three replicates.

■ RESULTS AND DISCUSSION

Con A is a tetrameric lectin protein that binds one α -glucopyranosyl (α DG) moiety at each subunit.²⁶ We selected Con A for this study because lectin proteins represent appropriate models for biosensing applications because of their ability to recognize specific carbohydrate bonding patterns. This ability has been used to engineer self-regulated insulin delivery systems,²⁸ demonstrating the value of Con A for future biomedical devices.²⁹ In addition, Con A is a relatively stable protein with respect to denaturation³⁰ and has been used previously to study protein adsorption on various surfaces.^{31–35} Our experimental approach is depicted in Figure

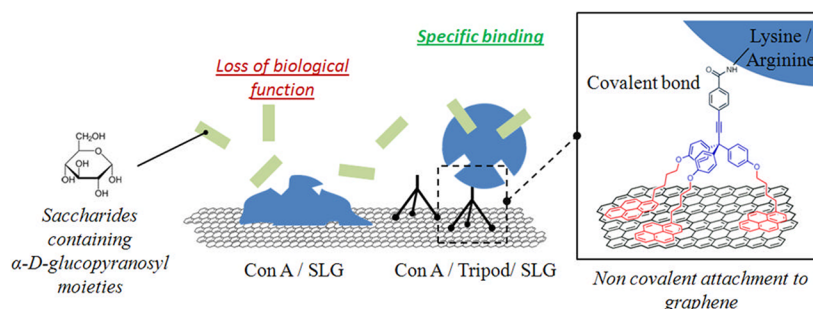


Figure 1. Schematic depiction of the strategies used to interface Concanavalin A to single-layer graphene and evaluate its carbohydrate-binding function.

1, in which we employed QCM to characterize films of Con A formed by physisorption onto bare SLG and by chemisorption onto tripod SAMs bearing amine-reactive NHS esters. Changes in resonant frequency (Δf) and motional resistance (ΔR) of the QCM measure the mass deposition and viscoelastic behavior, respectively, of the adsorbed films. Δf can be related to mass of Con A deposited on the quartz surface (Δm) using the Sauerbrey equation, assuming that the film is both uniform and rigidly coupled to the resonator surface:

$$\Delta f = -C_f \Delta m \quad (1)$$

C_f is a constant dependent on the quartz properties, $56.6 \text{ Hz } \mu\text{g}^{-1} \text{ cm}^2$ for the 5 MHz AT-cut quartz used here.³⁶ Figure 2

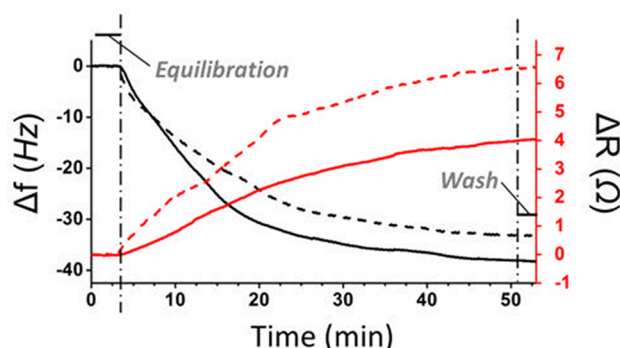


Figure 2. Changes in GQCM resonance frequency (Δf , left axis) and resistance (ΔR , right axis) upon introducing Con A into the flow cell. Two cases are compared: Con A immobilization onto bare SLG (Δf_a and ΔR_a , —) and covalent attachment to a monolayer of tripodal binding compound (Δf_t and ΔR_t , ---).

shows the GQCM responses for the functionalized and unfunctionalized resonators upon introduction of Con A. Although Con A deposits on both substrates, the mass and the viscoelastic properties of the resulting films differ. When Con A is adsorbed on bare graphene, Δf_a stabilizes after 30 min to $-38 \pm 1.2 \text{ Hz}$, corresponding to a mass of $671 \pm 21 \text{ ng/cm}^2$. Δf_t is slightly lower over the same period when the tripod monolayer is present, $-33 \pm 0.8 \text{ Hz}$, corresponding to an adsorbed mass of $583 \pm 14 \text{ ng/cm}^2$. These measurements indicate that more Con A deposits onto bare SLG than onto the tripod monolayer. Surface coverage calculations indicate that the mass of adsorbed Con A corresponds to 0.75–1.7 monolayers in the presence of the tripod monolayer and 0.85–2.05 layers for Con A adsorbed to bare SLG (see Supporting Information).

Under specific conditions satisfied in this study (see Supporting Information), changes in quartz motional resistance

(ΔR) correspond to variations in the acoustic impedance of the film deposited onto the quartz resonator.³⁷ The acoustic impedance provides insight into the film's viscoelastic properties, which for biological thin films depends on many factors, such as their degree of hydration.³⁸ Thus, differences in ΔR between films of Con A on bare SLG (ΔR_a) and on tripod SAMs (ΔR_t) qualitatively indicate differences in their physical properties and the nature of their solvent interactions. The film deposited by adsorption of Con A on bare graphene, in addition to containing more mass, is more rigid ($\Delta R_a = 4 \pm 0.6 \Omega$) than the film deposited on the tripod monolayer ($\Delta R_t = 6.6 \pm 0.8 \Omega$). This difference, in combination with the activity studies described below, is consistent with Con A interacting with SLG through its nonpolar amino acid residues. We associate this phenomenon with protein denaturation, which results in a more dense and rigid film compared to when it is covalently attached to the tripod SAM.³⁹

We next characterized Con A's ability to recognize α -D-glucopyranosyl or α -D-mannopyranosyl moieties in oligosaccharides to evaluate the adsorbed protein's level of function.⁴⁰ A flow of PBS 1X buffer solution was established over the Con A-functionalized GQCM cell until the frequency stabilized, after which a saturated solution of oligosaccharides containing α -D-glucopyranosyl moieties (PaDG) was introduced. A sudden decrease in the resonant frequency of about 5 Hz is first observed, consistent with a change in solvent viscosity (Figure 3).⁴¹ The resonant frequency continued to decrease over the next 30 min, corresponding to PaDG interacting with the Con A film. Finally, the cell is washed with PBS buffer, which reverses the initial 5 Hz shift related to the change in solvent viscosity. We observed a significant dependence of PaDG binding on the Con A attachment protocol (Table 1). Con A films that were attached to tripod monolayers underwent a GQCM resonant frequency shift of $-33.2 \pm 2.3 \text{ Hz}$, whereas the resonant frequency shift of Con A films adsorbed on bare SLG was only $-13.3 \pm 0.8 \text{ Hz}$. Nearly identical frequency shifts were observed when PaDG was introduced to Con A/tripod films when an acetate buffer solution was used in place of PBS 1X (see Supporting Information).

This activity difference between Con A on SLG and Con A on a tripod SAM cannot be explained by the protein simply adopting different orientations upon immobilization on the graphene surface, as no single orientation would restrict access to all four of Con A's α -D-glucopyranose binding sites. As such, we hypothesized that Con A retains its function when covalently attached to the tripod but denatures upon adsorption to bare SLG. To investigate this idea, we denatured the tripod-bound Con A by introducing a guanadine

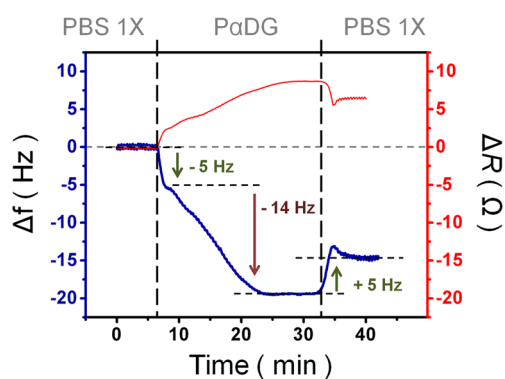


Figure 3. Time evolution of the GQCM resonance frequency (blue) and motional resistance (red) of an unfunctionalized GQCM during a PαDG binding experiment. The following solution sequence was introduced to the GQCM: PBS 1X equilibration ($t = 0-6$ min), PαDG solution ($t = 6-32$ min), PBS 1X washing ($t = 32-42$ min). The resonance frequency shifts associated with switching between PBS 1X and PαDG solutions (± 5 Hz) and nonspecific adsorption of PαDG to the GQCM (-14 Hz) are indicated.

hydrochloride solution (GdmCl, 6 M) into the flow cell before evaluating PαDG binding. The denatured Con A/tripod film, the adsorbed Con A/SLG film, and a pristine GQCM substrate each exhibited similar GQCM resonant frequency variation in the presence of PαDG (Table 1), which we attribute to nonspecific PαDG binding. Only the intact Con A/tripod film exhibits a larger resonant frequency shift than the nonspecific PαDG response. Figure 4 shows the QCM frequency response to PαDG exposure for each of these films. One notable feature is the loss of mass ca. 12 min for Con A adsorbed on bare SLG, which we attribute to the desorption of additional Con A nonspecifically bound to the protein monolayer,^{42,43} thus contributing to the net decrease of mass. Furthermore, the frequency response of the Con A/tripod films is an order of magnitude too large to correspond simply to the mass of bound oligosaccharides (see Supporting Information). We attribute this non-Sauerbrey response to a change in aggregation state of Con A upon PαDG binding, which has been noted previously in the presence of polyvalent oligosaccharides.⁴⁴

We further confirmed that the PαDG binding observed for tripod-supported Con A is attributable to an intact, functioning protein using an inhibition experiment developed by Doyle and Birdsell for Con A in solution.⁴⁵ This experiment exploits Con A's ability to specifically recognize α -D-mannopyranosyl residues of lipotechoic acids, which are located on the cell walls of gram-positive *B. subtilis* bacteria. We measured the density of *B. subtilis* cells that bound to Con A films, which were either adsorbed onto bare SLG (Figure 5, green bars) or attached to the tripod monolayer (Figure 5, yellow bars). Approximately five times more *B. subtilis* cells bind to the Con A/tripod films per unit area ($4826 \pm 1030 \text{ mm}^{-2}$, orange bars) than the adsorbed Con A films ($911 \pm 449 \text{ mm}^{-2}$, green bars). This difference is consistent with the results of the PαDG GQCM binding studies described above. Con A/tripod films

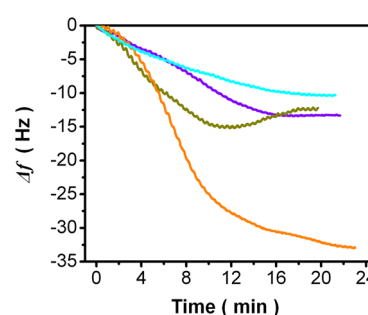


Figure 4. Time evolution of the GQCM resonant frequency after introducing the PαDG solution to bare SLG (purple), Con A adsorbed on bare graphene (green), Con A bound to tripod (orange), and denatured Con A bound to tripod (cyan).

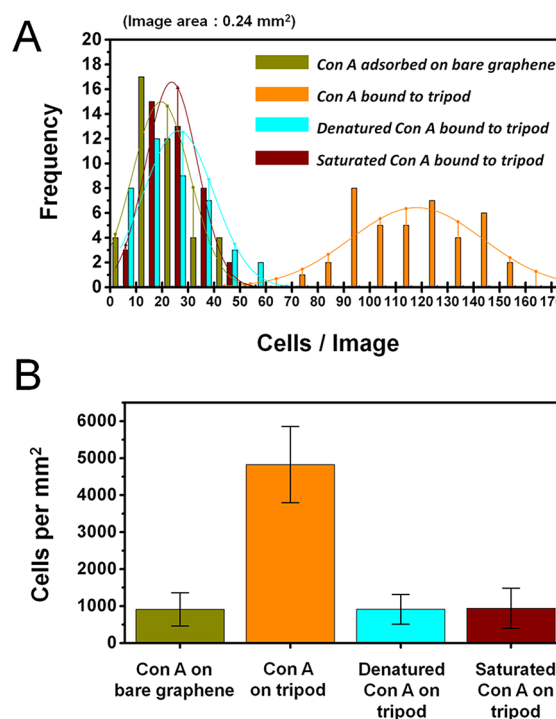


Figure 5. (A) Histogram of *Bacillus subtilis* cell density (image field of view = $24\,418 \mu\text{m}^2$) bound to SLG functionalized as follows: Con A adsorbed onto SLG (green bars); Con A bound to the tripod monolayer (orange bars); Con A bound to the tripod monolayer and then denatured with GdmCl solution (red bars); Con A bound to the tripod monolayer and then saturated with a methyl α -D-mannopyranoside solution (cyan bars). Normal distribution curves centered on the mean cell density values are overlaid onto each data set. (B) Surface densities of *Bacillus subtilis* cells (cells/mm^2) bound to SLG for the above surface preparation protocols. The data presented in this figure and the calculated mean cell densities were obtained from three replicate surfaces of each experiment (41 images cumulated for each experiment).

that were denatured, again using 6 M GdmCl, reduced the bound *B. subtilis* cell density ($913 \pm 401 \text{ mm}^{-2}$, Figure 5, cyan

Table 1. Binding of PαDG on Various GQCM Substrates^a

	pristine SLG	Con A adsorbed on SLG	Con A attached to tripod	denatured Con A attached to tripod
resonance frequency shift (Hz)	-12.9 ± 1.3	-13.3 ± 0.8	-33.2 ± 2.3	-11.5 ± 1.1

^aThe resonance frequency shift associated with the binding of PαDG to Con A-conjugated single layer graphene (error bars are $\pm\sigma$). As a negative control, the resonance frequency shift associated with introducing the PαDG solution over bare SLG is displayed.

bars) to a level similar to that of the adsorbed Con A. Finally we inhibited Con A function by saturating the binding sites of the active Con A/tripod films with methyl α -D-mannopyranose prior to introducing the *B. subtilis* cells. Under these conditions, the *B. subtilis* cell density was reduced by 83–100% ($941 \pm 543 \text{ mm}^{-2}$, Figure 5, red bars) to a similar level as the nonspecific binding observed for denatured or adsorbed Con A. The results of this inhibition experiment further confirm that the Con A protein retains its function when covalently attached to the tripod SAM. Collectively, these cell recognition experiments illustrate the importance of engineering the protein/graphene interface in order for proteins to retain their higher order structure and function.

CONCLUSIONS

This study has demonstrated through complementary QCM and cell binding studies that the lectin protein Con A readily adsorbs to graphene but loses its ability to recognize oligosaccharides. The viscoelastic properties of these adsorbed Con A films are also consistent with a physisorption mechanism driven by changes in Con A's structure. In contrast, Con A retains its function when it is covalently tethered to a monolayer of a tripodal compound, which binds to graphene through noncovalent interactions. These findings demonstrate that the QCM is a powerful tool to study protein adsorption and function on graphene as this material begins to fulfill its outstanding technological promises. Given that Con A is relatively stable with respect to denaturation, these findings are likely to be applicable to a broad range of other less-stable proteins. Our results emphasize that adsorption to bare SLG, or even to monovalent pyrene anchors, may be an ineffective biofunctionalization strategy, and that protein function should be demonstrated unambiguously in such cases. In contrast, the tripodal NHS-ester used in this study preserves Con A function and represents a general approach to interface proteins to SLG. We are currently performing studies in which graphene's desirable electronic properties enable electronic sensing simultaneously with QCM mass and dissipation measurements.

ASSOCIATED CONTENT

Supporting Information

Additional details, figures, and tables. This material is available free of charge via the Internet at <http://pubs.acs.org>.

AUTHOR INFORMATION

Corresponding Author

*E-mail: ta232@cornell.edu (T.A.); wdichtel@cornell.edu (W.R.D.).

Author Contributions

The manuscript was written through contributions of all authors. All authors have given approval to the final version of the manuscript.

Notes

The authors declare no competing financial interest.

ACKNOWLEDGMENTS

We thank Dr. David Latulippe for helpful discussion on protein denaturation and Dr. Cynthia Kinsland for advice on the bacteria sample preparation. This research was supported through a grant from the National Science Foundation under ECCS-1001742 and through support from Analog Devices.

W.R.D. acknowledges support from the Alfred P. Sloan Research Fellowship. J.A.M. acknowledges the Cornell Integrative Graduate Education and Research Traineeship (IGERT) Program in the Nanoscale Control of Surfaces and Interfaces supported by the National Science Foundation under NSF Award DGE-0654193, the Cornell Center for Materials Research, and Cornell University.

REFERENCES

- (1) Geim, A. K.; Novoselov, K. S. *Nat. Mater.* **2007**, *6*, 183–191.
- (2) Ohno, Y.; Maehashi, K.; Matsumoto, K. *J. Am. Chem. Soc.* **2010**, *132*, 18012–18013.
- (3) Haixin Chang, H.; Tang, L.; Wang, Y.; Jiang, J.; Li, J. *Anal. Chem.* **2010**, *82*, 2341–2346.
- (4) Mannoor, S. M.; Tao, H.; Clayton, J. D.; Sengupta, A.; Kaplan, D. L.; Naik, R. R.; Verma, N.; Omenetto, F. G.; McAlpine, M. C. *Nat. Commun.* **2012**, *3*, 763.
- (5) Lu, C.-H.; Yang, H.-H.; Zhu, C.-L.; Chen, X.; Chen, G.-N. *Angew. Chem., Int. Ed.* **2009**, *48*, 4785–4787.
- (6) He, S.; Song, B.; Li, D.; Zhu, C.; Qi, W.; Wen, Y.; Wang, L.; Song, S.; Fang, H.; Fan, C. *Adv. Funct. Mater.* **2010**, *20*, 453–459.
- (7) Cameron, J.; Wilson, C. J.; Clegg, R. E.; Leavesley, D. I.; Pearcy, M. J. *Tissue Eng.* **2005**, *11*, 1–18.
- (8) Gray, J. J. *Curr. Opin. Struct. Biol.* **2004**, *14*, 110–115.
- (9) Yanik, A. A.; Huang, M.; Kamohara, O.; Artar, A.; Geisbert, T. W.; Connor, J. H.; Altug, H. *Nano Lett.* **2010**, *10*, 4962–4969.
- (10) Lyu, Y.-K.; Lim, K.-R.; Lee, B. Y.; Kim, K. S.; Lee, W.-Y. *Chem. Commun.* **2008**, 4771–4773.
- (11) Wang, J. J. *Pharm. Biomed. Anal.* **1999**, *19* (1–2), 47–53.
- (12) Mohanty, N.; Fahrenholtz, M.; Nagaraja, A.; Boyle, D.; Berry, V. *Nano Lett.* **2011**, *11* (3), 1270–1275.
- (13) Lee, J. S.; Joung, H.-A.; Kim, M.-G.; Park, C. B. *ACS Nano* **2012**, *6*, 2978–2982.
- (14) Kodali, V. K.; Scrimgeour, J.; Kim, S.; Hankinson, J. H.; Carrol, K. M.; de Heer, W. A.; Berger, C.; Curtis, J. E. *Langmuir* **2011**, *27*, 863–865.
- (15) Haynes, C. A.; Norde, W. *Coll. Surf., B.* **1994**, *2*, 517–566.
- (16) Roach, P.; Farrar, D.; Perry, C. C. *J. Am. Chem. Soc.* **2005**, *127*, 8168–8173.
- (17) Nakanishi, K.; Sakiyama, T.; Imamura, K. *J. Biosci. Bioeng.* **2001**, *91*, 233–244.
- (18) Zougrana, T.; Findenegg, G. H.; Norde, W. *J. Colloid Interface Sci.* **1997**, *190*, 437–448.
- (19) Haynes, C. A.; Norde, W. *J. Colloid Interface Sci.* **1995**, *169*, 313–328.
- (20) Katoch, J.; Nyon, S. N.; Kuang, Z.; Farmer, B. L.; Naik, R. R.; Tatulian, S. A.; Ishigami, M. *Nano Lett.* **2012**, *12*, 2342–2346.
- (21) Mann, J. A.; Rodríguez-López, J.; Abruña, H. D.; Dichtel, W. R. *J. Am. Chem. Soc.* **2011**, *133*, 17614–17617.
- (22) Rodríguez-López, J.; Ritzert, N. L.; Mann, J. A.; Tan, C.; Dichtel, W. R.; Abruña, H. D. *J. Am. Chem. Soc.* **2012**, *134*, 6224–6236.
- (23) Mann, J. A.; Alava, T.; Craighead, H. G.; Dichtel, W. R. *Angew. Chem., Int. Ed.* **2013**, *52*, 1–5.
- (24) Li, X.; Cai, W.; An, J.; Kim, S.; Nah, J.; Yang, D.; Piner, R.; Velamakanni, A.; Jung, F.; Tutu, E.; Banerjee, S. K.; Colombo, L.; Ruoff, R. S. *Science* **2009**, *324*, 1312–1314.
- (25) Abergel, D. S. L.; Russel, A.; Falko, V. I. *App. Phys. Lett.* **2007**, *91*, 063125–063125–3.
- (26) Goldstein, I. J.; Hollerman, C. E.; Merrick, J. M. *Biochim. Biophys. Acta* **1965**, *97*, 68–76.
- (27) Sugisawa, H.; Edo, H. *J. Food Sci.* **1996**, *31*, 561–565.
- (28) Brownlee, M.; Cerami, A. *Science* **1979**, *206*, 1190–1191.
- (29) Qiu, Y.; Park, K. *Adv. Drug Delivery Rev.* **2001**, *53*, 321–339.
- (30) Chatterjee, A.; Mandal, D. K. *Biochim. Biophys. Acta* **2003**, *1648*, 174–183.
- (31) Diniz, F. B.; Ueta, R. R. *Electrochim. Acta* **2004**, *2S*, 4281–4286.
- (32) Mielczarski, J. A.; Dong, J.; Mielczarski, E. J. *Phys. Chem. B* **2008**, *112*, 5228–5237.

- (33) Gallinet, J.-P.; Gauthier-Manuel, B. *Eur. Biophys. J.* **1993**, *22*, 195–199.
- (34) Archambault, J. G.; Brash, J. L. *Colloids Surf., B.* **2004**, *25* (1–2), 9–16.
- (35) Gümüşderelioglu, M.; Agi, P. *React. Funct. Polym.* **2004**, *61*, 211–220.
- (36) Buttry, D. *Electroanalytical Chemistry*; Bard, A., Ed.; Marcel Dekker: New York, 1991; pp 23–33.
- (37) Geelhood, S. J.; Frank, C. W.; Kanazawa, K. *J. Electrochem. Soc.* **2002**, *149*, H33–H38.
- (38) Höök, F.; Rodahl, M.; Kasemo, B.; Brzezinski, P. *Proc. Natl. Acad. Sci. U.S.A.* **1998**, *95*, 12271–12276.
- (39) Rodahl, M.; Höök, F.; Fredriksson, C.; Keller, C. A.; Krozer, A.; Brzezinski, P.; Voinova, M.; Kasemo, B. *Faraday Discuss.* **1997**, *107*, 229–246.
- (40) Iyer, R. N.; Goldstein, I. *J. Immunochem.* **1973**, *10*, 313–322.
- (41) Auge, J.; Hauptmann, P.; Hartmann, J.; Rösler, S.; Lucklum, R. *Sens. Actuators, B* **1995**, *24–25*, 43–48.
- (42) Yuan, Y. J.; van der Werff, M. J.; Chen, H.; Hirst, E. R.; Xu, W. L.; Bronlund, J. E. *Anal. Chem.* **2007**, *79*, 9039–9044.
- (43) Johansson, T. *Affinity Measurements Using Quartz Crystal Microbalance (QCM)*; Springer: Berlin, 2010; pp 683–693.
- (44) Goldstein, I. J.; Hollerman, C. E.; Merrick, J. M. *Biochim. Biophys. Acta* **1965**, *97*, 68–76.
- (45) Doyle, R. J.; Birdsell, D. C. *J. Bacteriol.* **1972**, *652–658*.